Proceedings 20th NZ Geothermal Workshop 1998

INVESTIGATIONS OF THE ONSET OF SILICA SCALING AROUND CIRCULAR CYLINDERS

H.A. ZIPFEL[1], M.G. DUNSTALL[2] AND K.L.BROWN[2]

[1]University of Stuttgart, IHS, Germany.
[2]Geothermal Institute, The University of Auckland, Auckland, NZ

SUMMARY - The pressure distribution around a cylinder at different Reynolds numbers has been measured in a water tunnel, in which temperature and fluid velocity can be controlled. These pressure distributions are compared with published data for dynamically similar flows and related to silica deposition experiments around circular cylinders, which were carried out in the same water tunnel, under the same flow conditions. Silica scale thickness varies around the cylinder with the greatest deposition rate occurring, at least initially, in regions of high wall shear stress. Further experiments are planned to overcome slight flow variability experienced with the current configuration.

1. INTRODUCTION

Geothermal water contains dissolved silica, which can cause severe scaling problems in pipelines, reinjection wells and heat exchangers. Supersaturation of silica due to steam extraction and fluid cooling increases the likelihood of scale formation on equipment surfaces.

The main problems associated with silica scaling are increased pressure drop and blockages in pipelines and reinjection well casings, and reduction of heat transfer rates in heat exchangers.

A reduction in silica deposition rate has the potential to delay pipeline and heat exchanger replacement and reduces cleaning costs, as well as providing more efficient geothermal energy utilisation from higher useable temperature differences.

An apparatus has been designed to enable fundamental studies of the silica scaling process to be made under flow conditions similar to those found in typical geothermal developments. Specifically, the relationship between the silica deposition process and fluid hydrodynamics is explored in this work.

In this paper experiments to measure the pressure distribution around a circular cylinder at various Reynolds numbers are described. The measured pressure distributions obtained in this work are related to silica deposition experiments previously carried out on geometrically similar cylinders, in the same test rig. Ultimately, it is expected that these results will form part of a database to support numerical and analytical investigations of the silica scaling problem.

1.1 Previous experimental and numerical work

Garibaldi (1980) tried to determine the hydrodynamic effect on silica scaling in waste water drains at Wairakei. Two horizontal cylinders (axis perpendicular to the flow) and a flat plate (horizontal to the flow).were exposed for several weeks, showing that fluid hydrodynamics played an important role in the deposition process.

Higher rates of silica growth were observed in areas of low fluid velocity. For example, the stagnation line on an exposed cylinder showed a high rate of silica deposition. Less silica was observed at points of the highest velocity in the flow, occurring at 90° to the flow direction. The morphology of the silica scale was also found to be dependent on the flow condition. Cellular silica structures were observed in areas of recirculation, with fibrous structures in clearly directed flow. The exposed flat plates showed distinct silica deposition zones, which could be related to laminar and turbulent flow regions. However it was not possible to obtain uniform fluid flow or to clearly identify the flow condition, making it difficult to interpret these experiments or to compare them to other test data. In addition, there was no characterisation of the colloidal silica properties.

Rott et al. (1996) investigated silica deposition on to a flat plate using a numerical method. The governing equations of the fluid flow were modelled with PHOENICS, a commercial fluid flow software package, with force interactions between the particles and the fluid flow modelled in a particle tracking subroutine called GENTRA. Statistically, deposition of small

particles appeared much more likely than deposition of large particles, with an initial build-up at the front of the plate. It was predicted that this build-up would act as a tripping wire, promoting an earlier transition to turbulent flow conditions, which could increase colloidal deposition.

Recently, a test apparatus has been designed and commissioned at Wairakei by Dunstall and Brown (1998) to identify the hydrodynamic effect on the silica deposition process by controlling silica colloidal particle size and fluid flow conditions at the same time. Circular cylinders and flat plates were chosen for deposition experiments because of their well-examined hydrodynamic flow conditions. Test conditions in the apparatus represent those found in geothermal reinjection systems, since this is the predominant location for silica scaling problems. Particle size was varied from 10 nm to 100 nm, while velocity was adjusted from 0.5 m/s to 3 m/s. A more complete description of the test system is given by Dunstall and Brown (1998).

Very little scaling was observed on the flat plates, and it was not possible to relate results from the flat plate tests to any flow phenomenon. A series of six vertical mild steel cylinder experiments was carried out within a silica particle range of 25 nm to 125 nm and velocities ranging from 1 m/s – 2 m/s.

Scales observed on these cylinders were similar to those found in operational geothermal equipment, and showed a pronounced hydrodynamic effect. In this paper results from a vertical cylinder scaling test are related to pressure distribution tests recently carried out to characterise the flow.

2. THE TEST SECTION

The test apparatus used by Dunstall and Brown (1998) for earlier scaling tests was used for the current pressure distribution experiments around a circular cylinder. It consists of a 500 mm diameter settling section, which contracts smoothly and quickly down to a 200 mm diameter test section. A cylindrical bar, geometrically identical to those used in the previous silica deposition tests, was fitted with pressure taps. The cylinder diameter was 25 mm, giving a 16 % tunnel blockage ratio; tunnel blockage has an important influence on the pressure distribution results obtained. A cross-section of the cylinder used is shown in Figure 1.

Two radius-edged pressure tappings with a hole diameter of 0.5 mm were drilled in the mild steel cylinder, 90° apart. This arrangement provided two independent pressure readings as well as a means of orientating the pressure tappings with respect to the flow direction. Rotation and axial movement within the mounting ports was provided by a sliding fit through an O-ring seal; this allowed the pressure tappings to be positioned at any location across the width of the test section.

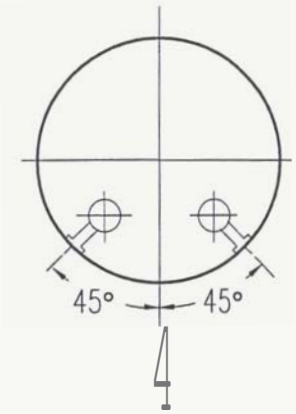

Figure 1 – Cross-section of test cylinder

Angle calibration was achieved by turning the cylinder until the pressure differential between the tappings was zero, while both tappings were connected to the same Rosemount pressure transducer (305 lCD-1 model).

Pressure variations over the cylinder surface were measured by taking the static pressure at the cylinder surface and subtracting the pipe wall static pressure, taken at the entrance of the test section. A Rosemount differential pressure transducer (3051CD-1 model), connected to a Campbell 21-X data logger was used to record these pressures. A three way valve provided a quick changeover between one of the cylinder tappings and the test section wall static pressure, which was used as the reference pressure for all measurements. This configuration is shown in Figure 2.

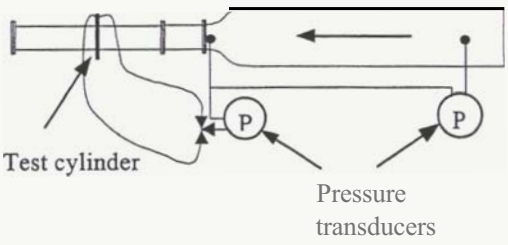

Figure 2 – Test section layout

A second differential pressure transducer, shown on the right side of Figure 2, was used for monitoring and controlling the flow velocity in the water tunnel. This transducer measures the static pressure differential between the test section and the stilling chamber.

A dimensionless pressure coefficient $C_P(\Theta)$ was used when evaluating the results:

$$C_P(\Theta) = \frac{p_{\Theta stat} - p_{wall}}{\frac{1}{2}\rho v_\infty^2} \qquad (1)$$

The local static pressure, measured at the cylinder wall at a tap angle Θ, is denoted $p_{\Theta stat}$. The reference static pressure at the pipe wall is denoted p_{wall}. The term in the denominator represents the free-stream dynamic water pressure (p_{dyn}) in the test section.

A drag coefficient C_D, for the pressure drag component, can be obtained by integrating the mean pressure distribution using the following expression:

$$C_D = \int_0^{2\pi} C_p(\Theta)\cos\Theta d\Theta \qquad (2)$$

3. THE FLOW *AROUND* A CIRCULAR CYLINDER

Many researchers, starting as early as von Kármán (1911-1912), have investigated flow phenomena around a circular cylinder. This body of work provides an established database for comparison with our pressure distribution results. Using measured pressure distributions we can identify the flow conditions in our test section and relate dynamically similar flows studied in other work to our silica deposition tests.

Here, we provide a brief introduction to boundary layer separation from a circular cylinder and the resulting pressure distribution. A more complete description of boundary layer flow is given by Schlichting (1979).

A cross section of flow around a vertical cylinder is shown schematically in Figure 3.

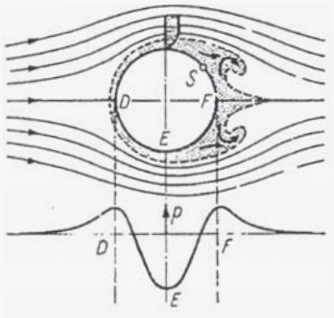

Figure 3 – Boundary layer separation around a circular cylinder (Schlichting, 1979)

Fluid particles are accelerated on the upstream half from D to E, and decelerated on the downstream half from E to F. As a result of the velocity changes, the pressure decreases from D to E and increases from E to F. Large friction forces in the thin boundary layer around the first half of the cylinder consume much of the moving particle's kinetic energy as it travels from D to E. The particle's remaining energy is then too small to surmount the "pressure hill" from E to F, and the particle is eventually arrested. The external pressure then causes it to move in the opposite direction, creating a recirculating wake zone.

In the Reynolds number range between Re = $1*10^4$ and Re = $6*10^6$ four flow regimes are commonly identified:

- subcritical flow regime
- critical flow regime
- supercritical flow regime
- transcritical flow regime.

As will be shown in the results, the subcritical and critical flow regime represent our flow conditions. Only these two flow regimes will be described in further detail.

Flow up to about Re = $1.2*10^5$ is characterised by purely laminar separation at about 80° from the stagnation line and is referred to as the subcritical flow regime. In this flow regime a drag coefficient (C_D) of about 1.15 is found. A minimum pressure coefficient (C_p) of around –1.2 and a base pressure coefficient (C_{pb}) of around –1.0 is experienced in this regime. The flow is characterised as being stable, hence the flow can be regarded as symmetrical.

An unstable flow regime at Reynolds numbers ranging from Re = $1.4*10^5 - 3.5*10^5$, called the critical flow regime, follows. Flow separation gradually shifts to higher separation angles up to 120°. This regime is characterised by a drop in C_D to a value of around 0.4. The minimum pressure coefficient C_p decreases to a value of about -2.5, the base pressure coefficient C_{pb} stays at –1.0. The unstable flow behaviour is characterised by a randomly changing boundary layer from laminar to turbulent separation at Reynolds number around Re = $2.8*10^5$, followed by a one-sided separation bubble which causes asymmetry in the pressure distribution. At the end of the critical range a two-sided separation bubble is experienced, which disappears with the onset of the supercritical regime.

The flow features described above are valid for a uniform flow around a smooth cylinder. Roughness height on the cylinder, tunnel blockage ratio, as well as free-stream turbulence, comprising of large and small scale turbulence, also have an impact on the separation mechanism of the flow around a cylinder.

Free-stream turbulence alters transitional behaviour such as mean drag, Strouhal number, mean pressure distribution, and the location of the separation point. In particular, small scale turbulence interacts with the boundary layer and

free shear layer, leading to an earlier transition of laminar to turbulent flow. As a result the separation line is shifted downstream as the turbulence intensity increases.

Surface roughness narrows the Reynolds number range of the flow regimes described earlier. This means that an earlier transition from laminar to turbulent flow conditions is promoted by high surface roughness.

It is generally recognised (E.S.D.U 1970) that the critical range of Reynolds numbers is narrower for high roughness and wider for high turbulence.

4. RESULTS

4.1 Initial experiments

Early tests showed encouraging results, but also identified some constraints with the current test equipment set-up.

Commissioning tests of the new cylinder showed slightly different pressure readings, depending on which of the two taps were used. The most likely cause of this variation lies in the manufacturing of the taps. The small holes were difficult to drill and one tap had to be relocated after breaking a drill bit. As the pressure readings from the two taps were inconsistent, an equalisation of the tapping pressure could not be used to calibrate tap-angle with respect to the flow direction. One tapping showed the same dynamic pressure at the stagnation line as the second Rosemount transducer, so this tapping was used for all further experiments and angle calibration. The separation distance between the pressure tappings was also found to be 88° instead of the designed 90°, but this is not expected to significantly influence the results obtained.

Accumulated silica scale partly blocked the heat exchanger, imposing a second constraint on the early experiments. A very large pressure drop (Δp=3.5 bar) was experienced between the heat exchanger inlet and the test section, resulting in very low flow rates (< 2 t/h) through the test rig. In order to maintain sufficient suction head to prevent pump cavitation, water flow through the rig had to be shut down. Unfortunately, this upset the energy balance in the test apparatus and a constant temperature could not be maintained in the circulating fluid. Heat transferred to the fluid by the pump was not transported out of the system and the steadily rising temperature reduced kinematic viscosity (v), and hence increased the Reynolds number according to equation (3).

$$Re = \frac{U_\infty \cdot d}{v} \qquad (3)$$

Here, U_∞ denotes the undisturbed free-stream velocity of the fluid and d the cylinder diameter.

4.2 Pressure distribution experiments

During the pressure distribution tests an attempt was made to reproduce the flow conditions prevailing in each of the previously conducted silica deposition experiments. Temperature increases during the tests did, however, alter the Reynolds number slightly.

For this study a silica scaling test cylinder, exposed to the circulating water flow for 34 days, with silica particles of 125 nm diameter, at a Reynolds number of Re = $1.07*10^5$, was studied. Flow conditions were determined fiom a pressure distribution test conducted over the Reynolds number range Re = 8.00 – $9.31*10^4$. Averaged experimental data from this test is displayed as a thick solid line in Figure 4.

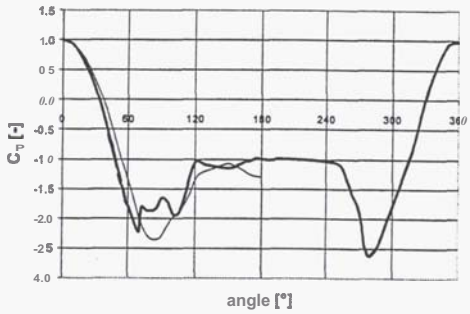

Figure 4 – Pressure coefficient vs. tap angle
—— Measured C_P at Re = 8 – **9.3*10⁴**;
—— Kwok (1986) data at Re = $8.31*10^4$

Our data is compared with experimental test data from Kwok (1986) which is shown as a thin solid line in Figure 4. His experiments were carried out with a tunnel blockage ratio of 12.5% and a rod-generated turbulence intensity of 9%. Kwok (1986) exposed only one side of the cylinder to free-stream turbulence, because he expected the flow to be symmetrical.

The fluctuations of the pressure coefficient C_P in our data between 70" and 100° are possibly due to a laminar separation bubble which flattens out the rising pressure distribution. A similar distribution is found in Flachsbart (1929). Apart from that, Kwok's values deviate only marginally from our experimental data. The increasing deviation towards 70° can be explained by the 3.5% higher tunnel blockage ratio in our experiments; this decreases the pressure coefficient C_P with increasing cylinder angle.

A Reynolds number in the range Re = 8.0 – $9.3*10^4$ suggests the flow is in a subcritical flow regime. However, the values of C_{pmin} = -2.4 and C_p = -1.0 as well as a drag coefficient (C_D = 0.54) indicate a critical flow regime rather than a subcritical one. Another indication for a critical flow regime is the asymmetric pressure distribution, which is commonly regarded as an indication of a one-sided laminar separation

bubble regime and usually observed in the critical flow regime.

The most likely reason for an early transition from laminar to turbulent flow conditions, as indicated by the measured pressure distribution, is small-scale turbulence in the flow. Small-scale turbulence is often responsible for altered transitional behaviour, as mentioned in section 3. Currently, the turbulence intensity in our test apparatus has not been measured. However, a turbulence intensity level similar to Kwok's (1986) results is expected, and will be verified by measurements after a heat exchanger clean out is complete.

4.3 The silica deposition hypothesis

Silica scale which formed on the cylinder exposed during earlier tests (34 days exposure, average particle *size* 125nm, $Re = 1.07*10^5$) is shown in Figure 5. A visual examination of this cylinder suggests a hydrodynamic effect in the silica deposition process. Firstly, no silica scale is observed at the stagnation line and, secondly, a non-uniform silica distribution around the cylinder is observed which relates closely to the asymmetric pressure distribution seen in Figure 4. The issue of asymmetry will not, however, be further examined in this paper.

The pressure coefficient data shown in Figure 4 confirm that the stagnation line is the region of highest pressure and hence lowest velocity in the boundary layer around the cylinder; it also has the highest streamline curvature. This result suggests that silica scaling with these colloid particles is less likely in regions with high and uniform streamline curvature. Stream lines are shown schematically in Figure 3 where the flow is directed towards the stagnation line.

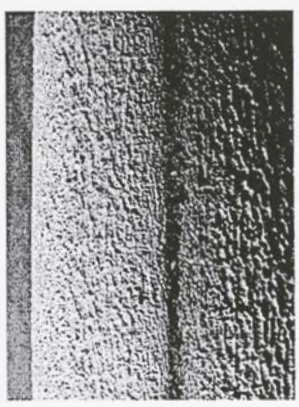

Figure 5 – Silica distribution around a cylinder at the stagnation line
($Re = 1.07*10^5$, particle size: 125nm)

On the front part of the cylinder the silica scale forms in rows, normal to the flow direction. A microscopic investigation of the silica layer revealed that row height varied with the cylinder angle. This distribution is shown in Figure 6. A sharp increase in row height can be seen up to 20° from the stagnation line, after which the scale thickness gradually decreases until 94° of angle is reached. At greater angles, which can be identified as being close to the separation angle, hardly any silica scale can be found on the cylinder surface.

Assuming that the silica deposition process is a function of time, the onset of silica precipitation must occur at the point of greatest accumulated silica height. Between 20" and 40" a "silica hill" is seen in Figure 6.

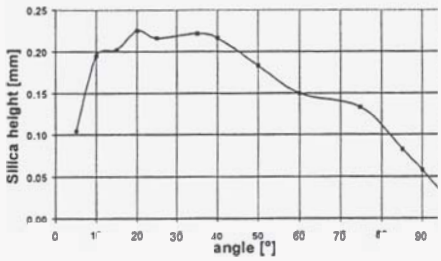

Figure 6 – Silica height over the circumference of a 25 mm test cylinder
($Re = 1.07*10^5$, particle size: 125 nm)

Referring to Figure 4, the angle of the steepest slope in the pressure coefficient C_P coincides with the "silica hill". Furthermore, the highest shear stress at the surface of a cylinder, in a flow at a Reynolds number of $Re = 2.6*10^5$, is found at an angle of 20°.

In our existing experimental set-up shear stress measurements could not be carried out. Nevertheless, after an extensive literature search a link between the shear stress coefficient and measured skin friction at a Reynolds number of $Re = 2.6*10^5$ has been established (Achenbach, 1968). The skin friction coefficient is defined as follows:

$$C_f = \left(\frac{\tau_0}{\rho U_\infty^2}\right)\sqrt{Re} \qquad (4)$$

where τ_0 is the shear stress. It is legitimate to use this data for comparative purposes since turbulence intensity shifts the actual Reynolds number to a potentially higher one, which is believed to be in the same flow regime, as discussed in the previous section.

Schlichting (1979) shows that the shear stress can be determined by differentiating the skin friction function. Hence to graphically determine the highest shear stress, tangents to the skin friction curve in Figure 7 have to be drawn. A high positive gradient of skin friction tangent corresponds to a point of peak shear stress. Therefore, the tangents at 25° and 335°

indicate maximum shear stresses, which corresponds well to the observed "silica hill".

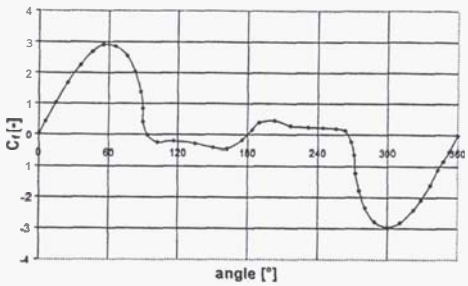

Figure 7 – Skin fiction distribution around a circular cylinder at Re = $2.6*10^5$ (Achenbach, 1968)

So far, a suitable model for precipitation of silica scale at the point of highest shear stress has not been developed but one explanation is that particles are "ripped off' the thin shear layer surrounding the cylinder due to high kinetic energy and adhere to the cylinder surface by London van der Waals forces.

5. CONCLUSIONS AND OUTLOOK

Preliminary pressure distributions tests have shown that silica precipitates more quickly in a region with high wall shear stress. However, several experiments have to be repeated under stable temperature conditions to verify these findings. Further information on the turbulence intensity in the test section is required to fully characterise the flow and to confirm the link between our results and independent research data for flows around cylinders. Measurements are planned to confirm this level of small scale turbulence, which is thought to be responsible for an early transition between flow regimes. The existing hypothesis for silica scale deposition has to be extended, and the asymmetry in the deposition investigated.

Ultimately, it is hoped that data obtained in this work will contribute to development of a complete silica deposition theory and allow numerical simulation of the silica scaling process.

6. ACKNOWLEDGMENTS

We thank the Foundation for Research Science and Technology for financial support, Lew Bacon and Contact Energy Ltd for financial and logistic support. Eddie Mroczek of IGNS deserves thanks for "minding" the apparatus from time to time. Discussions with Derek Freeston were always useful and appreciated.

7. REFERENCES

Achenbach, E. (1968). Distribution of local pressure and skin friction around a circular cylinder in cross-flow up to ***Re* = 5*10^6^, *Journal of Fluid Mechanics,*** Vol. 34, part 4, pp. 625-639

Dunstall, M.G. and Brown, K.L. (1998). Silica scaling under controlled hydrodynamic conditions. ***Proc. of 23rd Workshop on Geothermal Reservoir Engineering,, Stanford University, California, SGP-TR-158***

E.S.D.U. 1970 ***Engineering Science Data Item, No. 70013, Engineering Sciences Data Unit***

Garibaldi, F. (1980). The effect of some hydrodynamic parameters on silica deposition. ***Diploma Project*** *80.11*, ***Geothemzal Institute, University of Auckland.***

Flachsbart, O. (1929). From Roshko, A. (1961) Experiments on the Flow Past a Circular Cylinder at very high Reynolds Number; ***Journal of Fluid Mechanics,*** Vol. 10, pp. 345-356

von Kármán, Th. (1911-1912). Über den Mechanismus des Widerstandes, den ein bewegter Koper in Flussigkeiten erzeugt. *Nachr. Ges. Wiss. Gottingen, Math. Phys. Klasse,* pp. 509-517 and pp. 547-556.

Kwok. C.S.K. (1986). Turbulence effect on flow around circular cylinder. ***Journal of Engineering Mechanics,*** Vol. 112, No. 11, pp. 1181-1197

Pott, J., Dunstall, M.G. and Brown, K.L. (1996). Numerical simulation of silica scaling. ***Proc. of 18th New Zealand Geothermal Workshop,*** pp. 41-46.

Schlichting, H. (1979). Boundary-Layer Theory. ***McGraw-Hill*** Book Co. ***New York***